Intervertebral disc degeneration and changes in solute transport mechanisms in disc endplates studied by DCE-MRI

L.Tugan Muftuler[1], Joshua J. Jarman[2], Hon J. Yu[3], Dennis J. Maiman[4], and Vance O. Gardner[5]

[1]Department of Neurosurgery and Center for Imaging Research, Medical College of Wisconsin, Milwaukee, WI, United States, [2]Medical college of Wisconsin, WI, United States, [3]Radiological Sciences, University of California, Irvine, CA, United States, [4]Department of Neurosurgery, Medical college of Wisconsin, Milwaukee, WI, United States, [5]Orthopedic Research Institute of California, CA, United States

Target Audience: Clinicians and researchers interested in learning the pathophysiology of spinal disc degeneration

Introduction: Although intervertebral disc degeneration is a part of natural aging process, there are factors that influence the rate of degeneration. One of the proposed mechanisms is disruption of nutrient delivery through the disc endplates, which could lead to changes in cell biology, resulting in changes in biomechanical properties[1]. Thus, our main goal was to develop a clinically feasible Dynamic Contrast Enhanced MRI (DCE-MRI) protocol to study solute transport mechanisms in the endplates of degenerating discs. DCE-MRI enhancement in the cartilaginous endplates (CEP) and adjacent bony endplates (BEP) were studied using a high spatial resolution acquisition scheme. Secondly, we developed a quantitative MRI biomarker that is sensitive to various pathological changes during the course of disc degeneration. Such biomarkers are needed to study the association between changes endplate dynamics and ongoing degenerative processes.

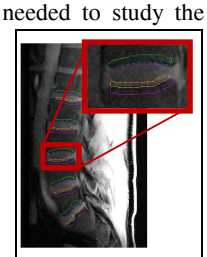

Fig.1. ROIs

Methods: Data were acquired from 8 subjects (age: 27–61y; mean 43y) using a 3T Philips scanner (Best, Netherlands). The study was approved by the IRB and written consents were obtained from subjects. 3mm thick, 15-sagittal slices were collected for each scan. A T2 weighted (T2w) MRI was acquired for grading of disc degeneration as per Pfirrmann *et al.*[2] Diffusion Weighted Images (DWI) were acquired to generate ADC maps for quantitative assessment of discs. A single-shot, spin-echo EPI sequence was used with TR/TE=4000ms/66ms, NEX=7, 2.4mm in plane resolution, b=600sec/mm^2 and one reference image. DCE-MRI was acquired using a 3D gradient-echo sequence (TR/TE=3.4ms/1.2ms, flip-angle=30^o, 0.81mm in-plane res. 22 frames/36.4s frame rate). The contrast (Gd-DTPA-BMA, 0.1 mmol/kg) was administered as a bolus via an antecubital vein at the start of the 3rd dynamic frame. For analysis, a trained operator drew regions of interest (ROI) on pre-contrast images of the DCEMRI set to segment out the 10 CEPs and BEPs in the lumbar area (Fig.1). The ROI-averaged DCE-MRI signals were normalized into percentage enhancement with respect to the mean of 2 pre-contrast dynamic frames. For quantitative assessment of degeneration, we proposed that ADC variations in the disc represent different stages of degeneration within the same Pfirrmann grade (PG). Thus, each disc was assigned a Degenerative Score (DS) that was within ±0.5 of its PG (Eq.1). In this equation, min_{ADC} and max_{ADC} are the minimum and maximum ADC values among discs only grouped within that particular PG, respectively.

$$DS(disc_n) = PG - \frac{ADC(disc_n) - min_{ADC}}{max_{ADC} - min_{ADC}} + 0.5 \qquad (1)$$

Results and Discussion: Fig.2 depicts DCE-MRI time course from the BEP and the CEP regions, which are averaged across the 80 BEPs and CEPs from the 8 subjects. The DCE-MRI time courses were remarkably different between the BEPs and adjacent CEPs. This could be expected since the contrast agent delivery mechanisms in the vascular BEPs and avascular CEPs are fundamentally different. When the subject lies in supine position, osmotic swelling pressure in discs is dominant and the endplates show low resistance to inflow.[3] This results in relatively fast fluid flow into the discs, transporting large molecular weight solutes to the disc. This might explain both the relatively fast appearance of contrast agent in the CEPs and also the sustained enhancement without noticeable washout. Another interesting finding was that the enhancement in CEPs increased by Pfirrmann grade (Fig.3). A one-way ANOVA analysis showed significant increase in area-under-enhancement-curve (AUC) with Pfirrmann grades ($p<0.0001$). Pairwise comparisons using Tukey's test showed that the mean AUC difference was not significant between grade 2 and 3 discs. But the difference from grade 3 to grade 4 was highly significant ($p<0.0001$). Increased contrast agent delivery into the CEPs of degenerated discs suggests that there might be a disruption in the integrity of the adjacent BEPs. Several studies reported increased openings in BEPs around degenerated discs, which are attributed to development of cracks and fissures in the BEPs. Additionally, the magnitude of signal enhancement was typically higher in the caudal CEPs compared to cranial CEPs. There was a subtle increase in the AUC with degeneration in cranial endplates but the correlation was weak (Fig.4). In contrast, the AUC of the caudal endplates showed a significant increase with increasing DS ($p<0.0001$) (Fig.4). Increased difference with degeneration possibly indicates that disc degeneration might have a detrimental effect on one endplate more than the other. Although the enhancement was generally higher in the caudal CEPs in this subject population, some of the discs showed the opposite effect. It is possible that either endplate is equally likely to degenerate in the general population. Furthermore, the AUC difference between caudal and cranial endplates was higher at the lower discs ($p=0.0006$) (Fig.5). This supports earlier findings showing a correlation in spinal level and disc degeneration.

Conclusions: Solute transport mechanisms in the CEPs and BEPs of lumbar discs change significantly as the discs degenerate. These might affect proper delivery of nutrients and removal of waste products in degenerating discs, initiating or accelerating the degenerative processes.

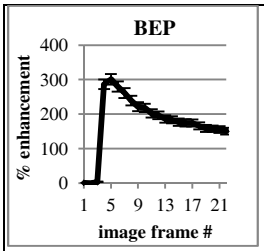

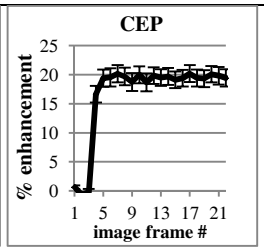

Fig.2. DCE-MRI signal in bony endplates (left) and cartilaginous endplates (right).

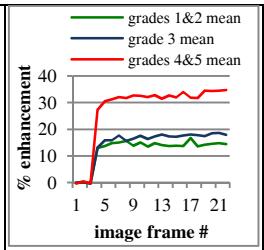

Fig.3. Enhancement in CEP with disc degeneration

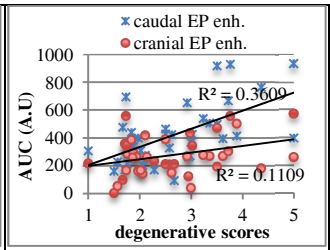

Fig.4. Cranial and caudal CEP enhancement by degenerative scores

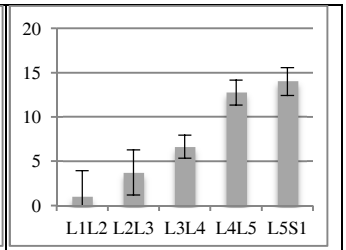

Fig.5. AUC difference between caudal and cranial CEP by level

References: [1] *An H, et al., Spine. 2004; 29(23): 2677-8*; **[2]** *Pfirrmann C. et al. Spine 2001, 26:1873-8*; **[3]** Ayotte DC, *et al*. J Orthop Res. 2001; 19(6): 1073-7.